

Low-Temperature Electronic Properties of the $\text{La}_{n+1}\text{Ni}_n\text{O}_{3n+1}$ ($n = 2, 3,$ and ∞) System: Evidence for a Crossover from Fluctuating-Valence to Fermi-Liquid-like Behavior

K. Sreedhar,* M. McElfresh,† D. Perry,‡ D. Kim,* P. Metcalf,* and J. M. Honig*

*Department of Chemistry, †Department of Physics, and ‡Department of Materials Engineering, Purdue University, West Lafayette, Indiana 47907

Received March 22, 1993; in revised form August 23, 1993; accepted August 25, 1993

Measurements of the temperature dependence of the electrical resistivity $\rho(T)$, magnetic susceptibility $\chi(T)$, and Seebeck coefficient $S(T)$ have been carried out on the $n = 2, 3,$ and ∞ members of the homologous lanthanum nickel oxide systems $\text{La}_{n+1}\text{Ni}_n\text{O}_{3n+1}$ that were annealed in air. With increasing n , a progressive decrease in the electrical resistivity and a gradual change from insulating to metallic behavior are observed. $\text{La}_3\text{Ni}_2\text{O}_7$ is nonmetallic, showing a gradual increase in ρ when T decreases ($d\rho/dT < 0$) from 300 to 4.2 K, whereas $\text{La}_4\text{Ni}_3\text{O}_{10}$ and LaNiO_3 exhibit metallic resistivity ($d\rho/dT > 0$). A minimum in $\rho(T)$ near 140 K is observed for $\text{La}_4\text{Ni}_3\text{O}_{10}$, while LaNiO_3 exhibits a T^2 dependence for $\rho(T)$ below ~ 50 K. The magnetic susceptibility of LaNiO_3 is Pauli-like, but the $\chi(T)$ data for $\text{La}_3\text{Ni}_2\text{O}_7$ and $\text{La}_4\text{Ni}_3\text{O}_{10}$ below 350 K show a decrease with decreasing temperature. The Seebeck coefficient of all these compounds is negative at high temperatures; $\text{La}_3\text{Ni}_2\text{O}_7$ and $\text{La}_4\text{Ni}_3\text{O}_{10}$ exhibit a sign change in S at low temperatures. These results suggest a crossover from a fluctuating-valence to a Fermi-liquid-like behavior with increasing n . © 1994 Academic Press, Inc.

I. INTRODUCTION

The electronic properties of mixed-valent oxides with perovskite and related structures, which exhibit insulator–metal (I–M) transitions as a function of composition or doping, are of great current interest. This is partly due to the occurrence of high T_c superconductivity in some of the copper oxide systems in this mixed-valent regime (1). In most of these cases, the I–M transition is achieved primarily by doping holes or electrons into the insulating parent compounds, which are thought to be Mott charge transfer type insulators.

The ternary nickel oxide system (La–Ni–O) is known to form a series of homologous compounds with the general formula $\text{La}_{n+1}\text{Ni}_n\text{O}_{3n+1}$ (2–5), whose structures are similar to those of the Ruddlesden–Popper series $\text{Sr}_{n+1}\text{Ti}_n\text{O}_{3n+1}$ (6). While the $n = 1$ member of this series (La_2NiO_4) exhibits a quasi-two-dimensional K_2NiF_4 -type structure,

the compound LaNiO_3 , which corresponds to the $n = \infty$ member of this series, assumes the three-dimensional distorted perovskite structure. The $n = 2$ and 3 members, corresponding to the formulas $\text{La}_3\text{Ni}_2\text{O}_7$ and $\text{La}_4\text{Ni}_3\text{O}_{10}$, have two and three perovskite-type (LaNiO_3) layers separated by a single rock-salt-type (LaO) layer, respectively. Hence, an increase in n is expected to increase the strength of the Ni–O–Ni interactions along the crystallographic c direction. The formal valence state of Ni varies from 2 for the $n = 1$ member to 3 for the $n = \infty$ member. For the intermediate members of this series Ni formally acquires a nonintegral valence between 2 and 3. This change in structure and valence state is expected to be reflected in the electronic properties of this homologous system.

Earlier electrical resistivity studies (7–10) have shown that La_2NiO_4 is a semiconductor with a conductivity activation energy of ~ 0.05 – 0.1 eV. This compound exhibits an I–M transition in the range 600–650 K when the current flow is directed along the basal plane. Consistent with its quasi-two-dimensional structure, the resistivity along the c direction is larger by two orders of magnitude than that in the basal plane. Electrical resistivity studies of polycrystalline compounds of the other members ($n = 2, 3,$ and ∞) have shown a decrease in the value of the room-temperature resistivity (ρ_{300}) and a change from semiconducting to metallic characteristics with an increase in n (11). The decrease in ρ with increase in n across this series was attributed by the authors to a decrease in the percolation threshold with the increasing three-dimensional character of these compounds.

We have carried out low-temperature (4.2–300 K) electrical resistivity $\rho(T)$, magnetic susceptibility $\chi(T)$, and Seebeck coefficient $S(T)$ measurements on the $n = 2, 3$ and ∞ members of the $\text{La}_{n+1}\text{Ni}_n\text{O}_{3n+1}$ series in order to investigate the effect of changes in structure and valence state of Ni on the electronic properties of the $\text{La}_{n+1}\text{Ni}_n\text{O}_{3n+1}$ system and to complement the available information on the $n = 1$ member, La_2NiO_4 .

II. EXPERIMENTAL

The $n = 2, 3,$ and ∞ members of the $\text{La}_{n+1}\text{Ni}_n\text{O}_{3n+1}$ series were synthesized by dissolving appropriate molar ratios of La_2O_3 (> 99.99% purity) and NiO (99.9% purity) in nitric acid and decomposing the nitrate mixture. The resulting product was pressed into pellets and heated in air for several days to 1150°C in the case of $\text{La}_3\text{Ni}_2\text{O}_7$, and to 1075°C in the case of $\text{La}_4\text{Ni}_3\text{O}_{10}$, with intermittent grinding and repelletization. The material was then cooled to room temperature at a rate of $\sim 2^\circ/\text{min}$. LaNiO_3 was synthesized as described previously (12).

X-ray powder diffraction patterns were recorded using a Siemens D-500 diffractometer with CuK_α radiation; they showed that the samples were single phase at this level of detection. Electron microscopic investigations were carried out using a Jeol 2000 EX electron microscope. Electrical resistivity measurements were made in the range 4.2–300 K on sintered bars using a standard four-probe technique. Magnetization measurements were performed on a Quantum Design SQUID magnetometer in the range $T = 4.2$ –350 K. Seebeck coefficient measurements were carried out in the range $T = 77$ –300 K via a standard temperature relaxation method.

III. RESULTS AND DISCUSSION

The schematic crystal structures of the $n = 1, 2,$ and ∞ members of the $\text{La}_{n+1}\text{Ni}_n\text{O}_{3n+1}$ series are shown in Fig. 1, which emphasizes the interleaving of the rock-salt-type (LaO) layers between n consecutive octahedral perovskite-type (LaNiO_3) layers. The $n = 2$ and 3 members can be thought of as having structures intermediate between the quasi-two-dimensional La_2NiO_4 ($n = 1$) and the three-dimensional perovskite LaNiO_3 ($n = \infty$) structures. Since the intermediate members of the series are very similar in crystal structure and thermodynamic stability, these compounds generally exhibit intergrowth of other members under ordinary preparative conditions (4, 11). However, such intergrowth can be minimized by annealing the samples at an optimized temperature (1150°C in the case of $\text{La}_3\text{Ni}_2\text{O}_7$ and 1075°C in the case of $\text{La}_4\text{Ni}_3\text{O}_{10}$) for several days. During the synthesis of the $n = 2$ and 3 members, La_2NiO_4 formation is generally observed prior to any appreciable formation of $\text{La}_3\text{Ni}_2\text{O}_7$ or $\text{La}_4\text{Ni}_3\text{O}_{10}$. This suggests that intergrowth of perovskite-type layers in the K_2NiF_4 -type structure is the likely mechanism for the formation of the higher members of this series, in conformity with a mechanism proposed earlier (5).

The X-ray powder diffraction patterns at room temperature of compounds $\text{La}_3\text{Ni}_2\text{O}_7$, $\text{La}_4\text{Ni}_3\text{O}_{10}$, and LaNiO_3 are shown in Fig. 2. These patterns indicate that at this level of detection the samples are single phase and crystallize in

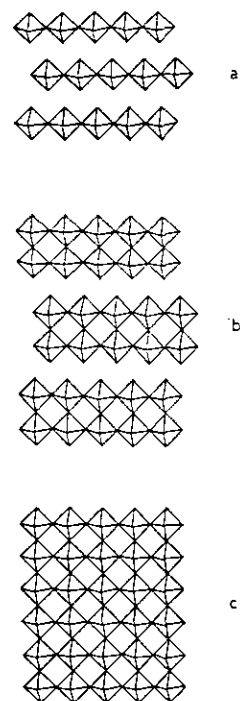


FIG. 1. Schematic representation of corner-linking of NiO_6 octahedra formulated for (a) $n = 1$, (b) $n = 2$, and (c) $n = \infty$ members of the $\text{La}_{n+1}\text{Ni}_n\text{O}_{3n+1}$ series.

the orthorhombically distorted Ruddlesden–Popper-type structure for the $\text{La}_3\text{Ni}_2\text{O}_7$ and $\text{La}_4\text{Ni}_3\text{O}_{10}$ compounds, and in a rhombohedrally distorted perovskite structure for LaNiO_3 . The X-ray diffraction patterns of the $n = 2$ and 3 members can be indexed as an orthorhombic unit cell, with lattice parameters $a = 5.41 \text{ \AA}$, $b = 5.46 \text{ \AA}$, $c = 20.54 \text{ \AA}$ and $a = 5.41 \text{ \AA}$, $b = 5.46 \text{ \AA}$, $c = 27.98 \text{ \AA}$, respectively. The X-ray powder diffraction pattern of LaNiO_3 can be indexed as a rhombohedral or, alternatively, as a hexagonal unit cell, with lattice parameters $a = 5.49 \text{ \AA}$ and $c = 13.14 \text{ \AA}$. These unit cell parameters agree within the experimental errors with those reported earlier (5, 11).

To monitor the extent of intergrowth of the intermediate members of the series, we have carried out high-resolution electron microscopic (HREM) studies on the $n = 2$ and 3 members (Fig. 3). As far as can be ascertained, we have been able to suppress intergrowth to a greater extent than was achieved in an earlier attempt (11), but this effect could not be completely eliminated. The HREM studies, which were carried out on only a tiny fraction of the sample, indicate that intergrowth occurs in these compounds only as isolated line defects in an otherwise nearly perfect lattice. Figure 3a for the $n = 3$ compound shows a reasonably perfect pattern; Fig. 3b for the $n = 2$ shows intergrowth of one additional perovskite layer, which suggests that any intergrowths will not significantly affect the electronic properties. These intergrowth defects are typical of this class of compounds and are similar to those

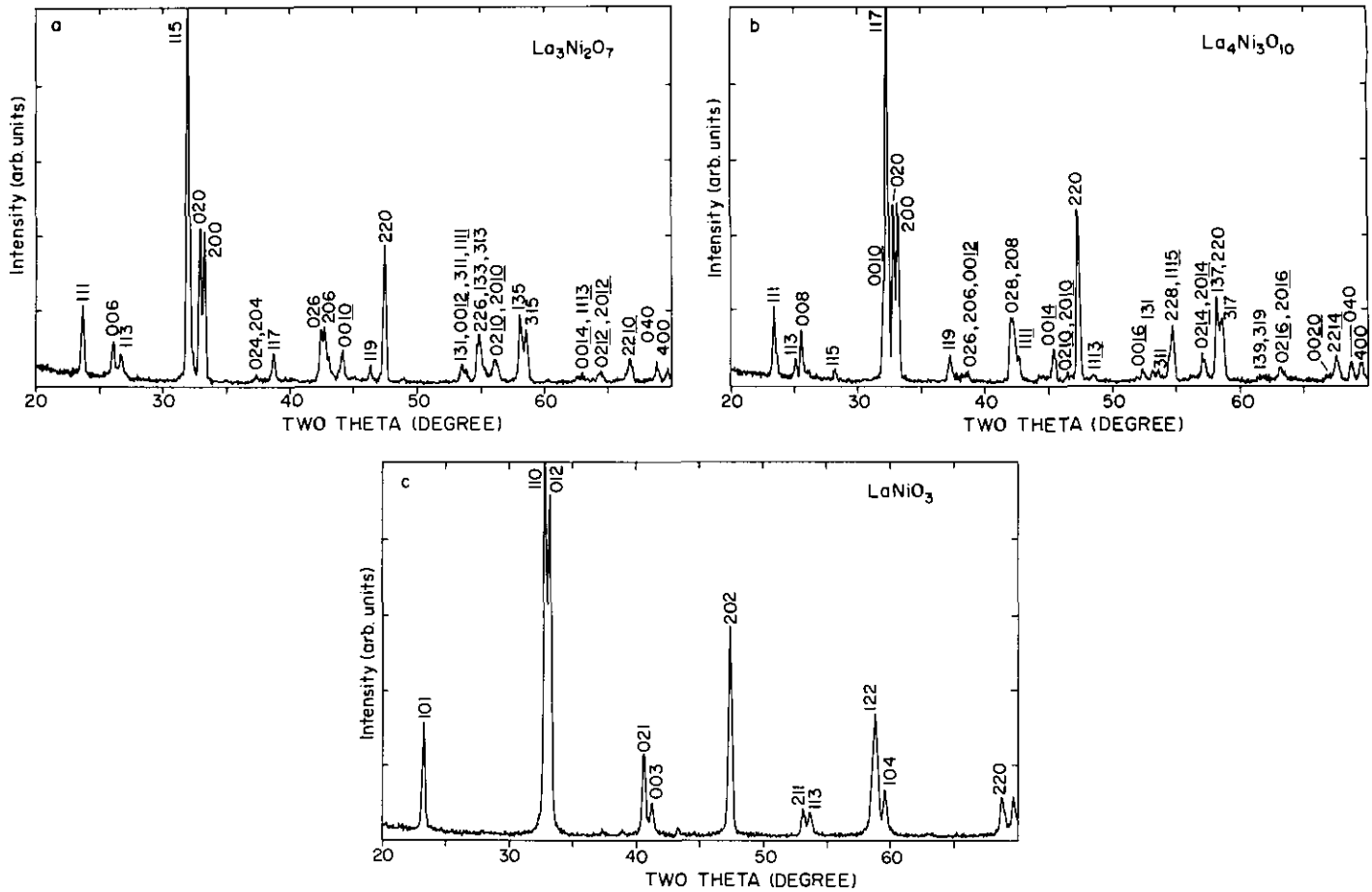


FIG. 2. X-ray powder diffraction patterns of (a) $\text{La}_3\text{Ni}_2\text{O}_7$, (b) $\text{La}_4\text{Ni}_3\text{O}_{10}$, and (c) LaNiO_3 obtained using CuK_α radiation.

observed in the high- T_c cuprate superconductors, for instance, in the $\text{Tl}_2\text{Ba}_2\text{Ca}_{n-1}\text{Cu}_n\text{O}_{2n+4}$ system (13), which shows a T_c as high as 125 K for the $n = 3$ member.

The temperature dependence of the magnetic susceptibility, $\chi(T)$, of the $n = 2, 3$, and ∞ members of the series is shown in Fig. 4. Earlier neutron diffraction and magnetic susceptibility studies on single crystals of the $n = 1$ member ($\text{La}_2\text{NiO}_{4+\delta}$) have shown that it orders antiferromagnetically, with T_N strongly dependent on δ (14–17). For the stoichiometric ($\delta = 0$) material the T_N is reported to be above room temperature. However, no magnetic ordering has been observed for the other members of this series. The susceptibility data of the $n = 2$ and 3 members below 350 K show a decrease with decreasing temperature and a minor increase in the susceptibility at the lowest temperatures. These results are somewhat at variance with earlier measurements (11); our values are a factor of roughly 2 lower than the χ values previously reported for the $n = 2, 3$ members, and the data of Mohan Ram *et al.* show a very sharp rise in χ with decreasing temperature for $T < 50$ K. In our measurements we have not encountered any large upturn in χ down to 4.2 K. This

latter magnetic behavior is qualitatively similar to that observed in rare-earth valence-fluctuating systems, for instance, in CeSn_3 (18), in the mixed valent vanadium oxide system $\text{V}_n\text{O}_{2n-1}$ (19–21), and in CuO (22), as well as in the quasi-two-dimensional $\text{La}_{2-x}\text{Sr}_x\text{NiO}_4$ system (23, 24) close to the composition range in which the compound changes from insulating to metallic characteristics. In the $\text{V}_n\text{O}_{2n-1}$ system, an antiferromagnetic interaction with short-range spin order and/or mixed-valent behavior of the vanadium ions has been invoked (20, 21) to explain the observed $\chi(T)$ behavior. In the case of $\text{La}_{2-x}\text{Sr}_x\text{NiO}_4$, the $\chi(T)$ data have been interpreted in terms of a large value of the antiferromagnetic exchange interaction and a high-spin to low-spin transition involving Ni 3d electrons (23, 24).

One possible interpretation of the $\chi(T)$ behavior of the $n = 2$ and 3 members of the $\text{La}_{n+1}\text{Ni}_n\text{O}_{3n+1}$ series is based on the two different valence states ($\text{Ni}^{2+}/\text{Ni}^{3+}$) of the transition metal with spin $S = 1$ and $S = \frac{1}{2}$, respectively, separated by an energy difference ΔE . A decrease in the population of the $S = 1$ excited state with a decrease in temperature would lead to a positive value of $d\chi/dT$. The

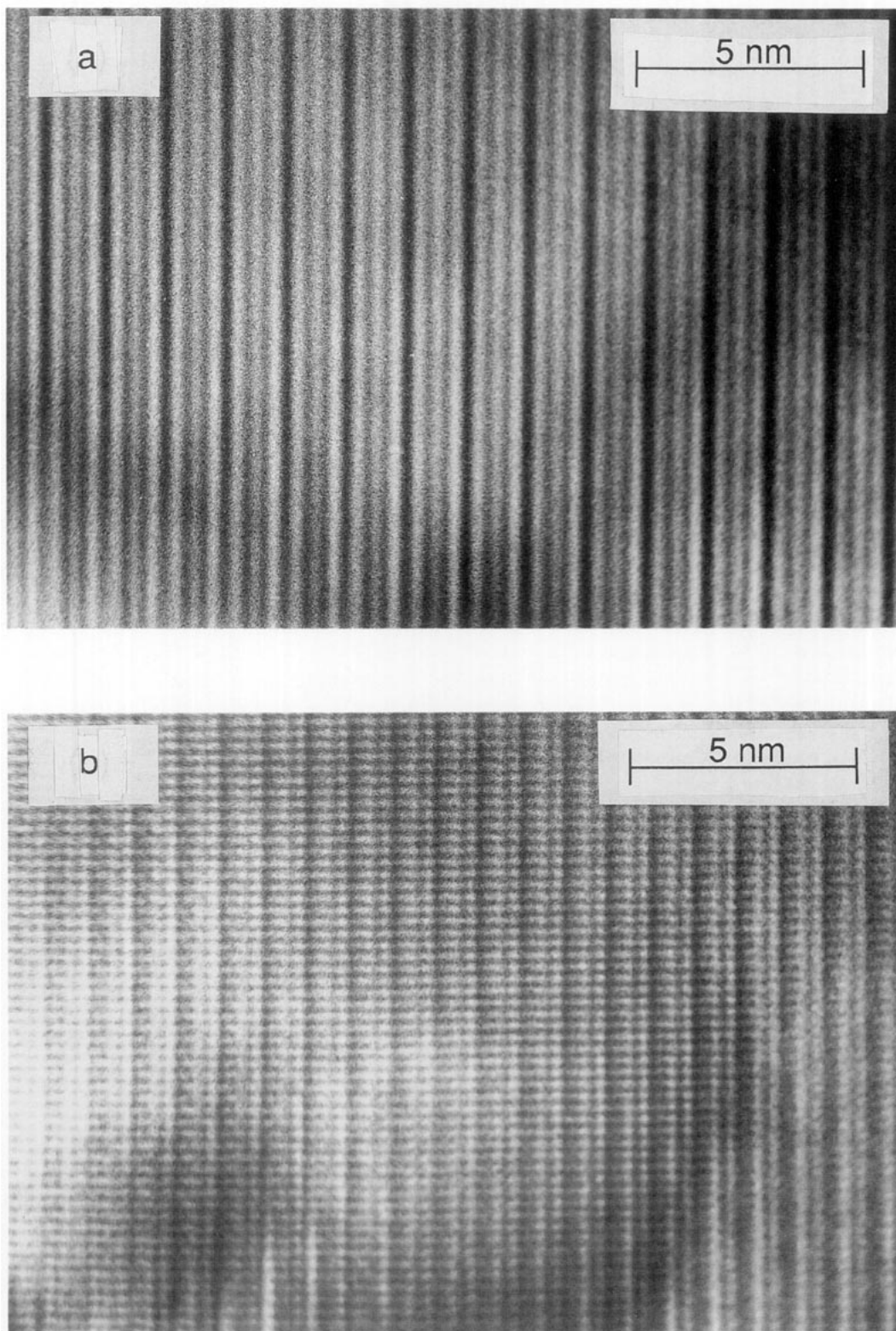


FIG. 3. Lattice image obtained along $\{\bar{1}10\}$ of (a) $\text{La}_4\text{Ni}_3\text{O}_{10}$ and (b) $\text{La}_3\text{Ni}_2\text{O}_7$.

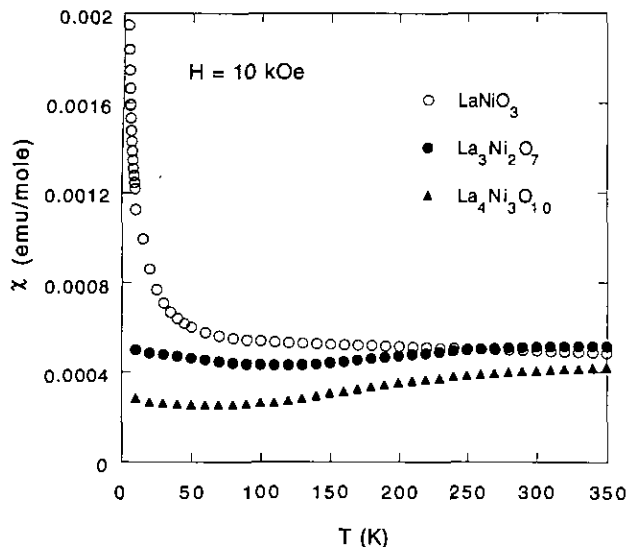


FIG. 4. Temperature-dependent magnetic susceptibility of $n = 2, 3$, and ∞ members of the $\text{La}_{n+1}\text{Ni}_n\text{O}_{3n+1}$ series.

opposite situation would prevail if Ni^{3+} were in the high-spin configuration. One should bear in mind, however, that this valence assignment is a formal one since it is by now generally accepted (25–30) that nickelates tend to be charge transfer insulators of the type first discussed by Zaanen *et al.* (31). In this picture the charge carriers would be primarily of O $2p$ character. The ultimate resolution of this problem for the present set of materials must await further careful studies of the band structure. Alternatively, the observed $\chi(T)$ behavior could be related to a large value of the antiferromagnetic exchange interaction energy (J) between the Ni ions, which has been invoked to explain rather similar $\chi(T)$ behavior observed in the $\text{La}_{2-x}\text{Sr}_x\text{NiO}_4$ system, for which J between Ni ions has been estimated to be of the order of 500–1000 K (23). In contrast to the $n = 2$ and 3 members, LaNiO_3 shows a nearly T -independent Pauli-like susceptibility in the range 50–350 K and a large increase in susceptibility at low temperatures (12), suggesting the presence of strong electron–electron interactions in this metallic narrow d -band system.

The temperature dependence of the electrical resistivity $\rho(T)$ of the $n = 2, 3$, and ∞ members of this series is shown in Fig. 5. The room-temperature resistivity (ρ_{300}) decreases from $\rho \sim 250 \text{ m } \Omega\text{-cm}$ for the $n = 2$ member to $\rho \sim 1.8 \text{ m } \Omega\text{-cm}$ for the $n = \infty$ member. Our results for LaNiO_3 are in good agreement with those reported in earlier investigations (11, 32–36), which indicates that resistivity studies on ceramic LaNiO_3 are fairly reproducible. Torrance *et al.* (29, 37) quote only resistances; when superposed on the other data their variation of ρ with T matches all others for $T < 150 \text{ K}$, but their ρ values

rise far more rapidly with $T > 150 \text{ K}$ than do all other experimental curves.

The T -dependence of the resistivity of the $n = 2, 3$, and ∞ members is qualitatively different. $\text{La}_3\text{Ni}_2\text{O}_7$, with a formal Ni valence of 2.5, exhibits nonmetallic electronic transport, with a gradual monotonic increase of $\rho(T)$ as the temperature is reduced from $T = 300$ to $T = 4.2 \text{ K}$. These findings are at variance with an earlier investigation involving $\text{La}_3\text{Ni}_2\text{O}_7$ with recurrent intergrowths of neighboring $\text{La}_{n+1}\text{Ni}_n\text{O}_{3n+1}$ homologs (11): in these studies $\text{La}_3\text{Ni}_2\text{O}_7$ was reported to be metallic with a nearly temperature-independent resistivity that was lower by a factor of 10 to 40 relative to the values shown in Fig. 5a. However, in the present study the T dependence of the resistivity at low temperatures does not follow an exponentially activated behavior, in contrast to La_2NiO_4 ($n = 1$), which does show an exponentially activated conduction (7, 10). $\text{La}_4\text{Ni}_3\text{O}_{10}$, which has a formal Ni valence of 2.67, exhibits metallic resistivity behavior but has a very shallow minimum in $\rho(T)$ close to 140 K. The data set displayed in Figure 5b is in quite good agreement with that reported by Mohan Ram *et al.* (11). For the $n = 2$ sample no minimum in resistivity has been observed in the range $T = 4.2\text{--}300 \text{ K}$. LaNiO_3 , with a Ni valence of +3, is metallic down to 4.2 K; the resistivity varies as T^2 below $T \sim 50 \text{ K}$.

The decrease in ρ_{300} with an increase in n across this series is consistent with an increase in the density of charge carriers. Since the number of adjacent perovskite-type layers rises with increasing n , an increase in Ni d -band width (W) is also expected, arising from an increase in Ni–O–Ni overlap along the crystallographic c direction. This decrease in ρ_{300} and the concomitant changeover from semiconducting to metallic-like behavior in this series are qualitatively similar to the I–M transition as a function of Sr doping observed in the quasi-two-dimensional $\text{La}_{2-x}\text{Sr}_x\text{NiO}_4$ system (23, 24, 38–40). In the latter case, a progressive changeover from insulating to metallic-like behavior is encountered when the Sr concentration exceeds $x = 0.90$. The nonmetallic electronic transport behavior of $\text{La}_3\text{Ni}_2\text{O}_7$, as well as the observed resistivity minimum close to 140 K for $\text{La}_4\text{Ni}_3\text{O}_{10}$, suggests the presence of strong electron–electron and conduction-electron localized magnetic moment scattering. However, the presence of a small degree of lattice disorder and/or nonstoichiometry, or a possible structural distortion, may also affect the low-temperature transport properties of these compounds.

The Seebeck coefficient data, $S(T)$, of the $n = 2, 3$, and ∞ members of the $\text{La}_{n+1}\text{Ni}_n\text{O}_{3n+1}$ series are shown in Fig. 6. The Seebeck coefficients reported here for LaNiO_3 agree well with those reported by Rajeev *et al.* (34, 36). As far as could be ascertained, there are no prior measure-

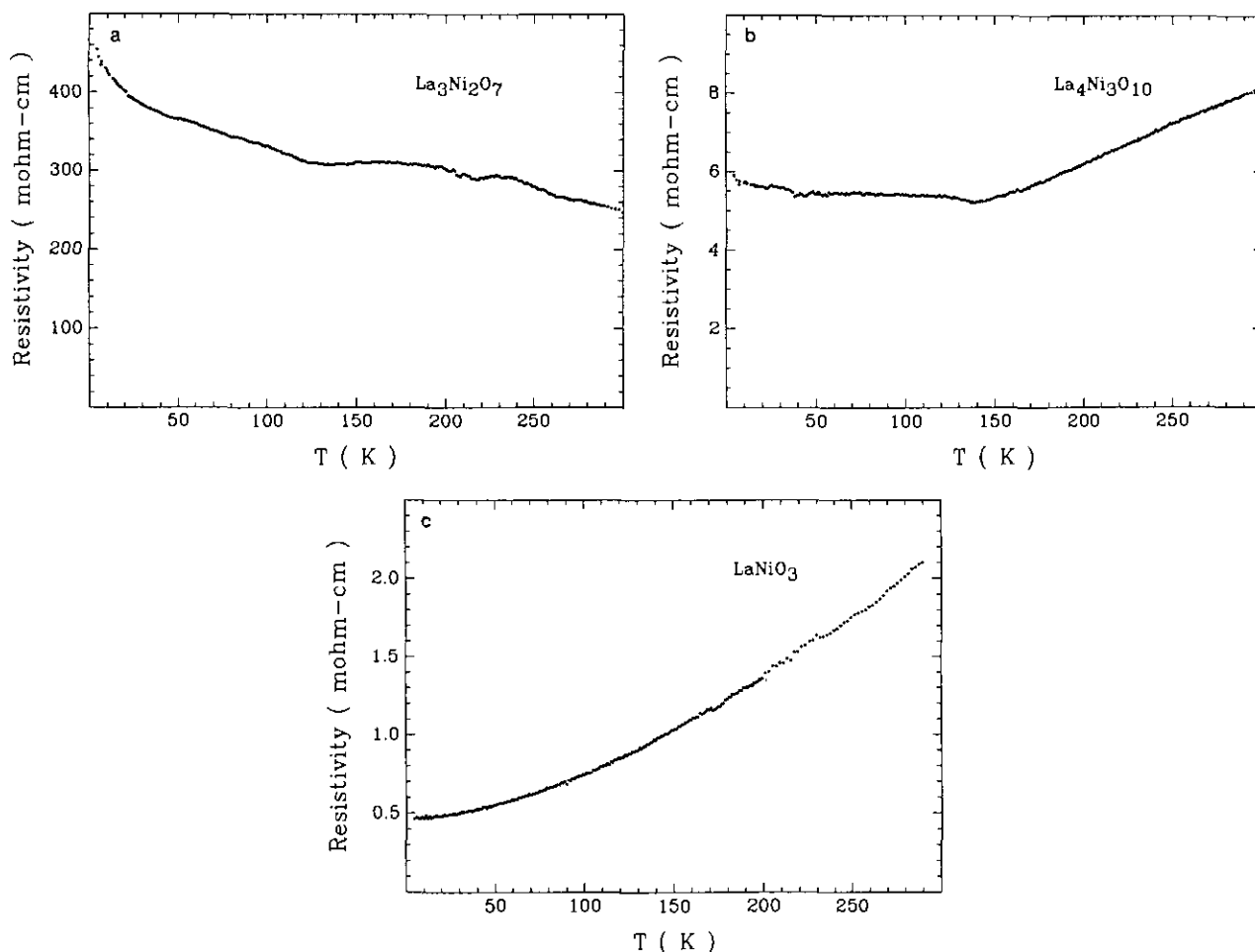


FIG. 5. Temperature-dependent electrical resistivity of (a) $\text{La}_3\text{Ni}_2\text{O}_7$, (b) $\text{La}_4\text{Ni}_3\text{O}_{10}$, and (c) LaNiO_3 .

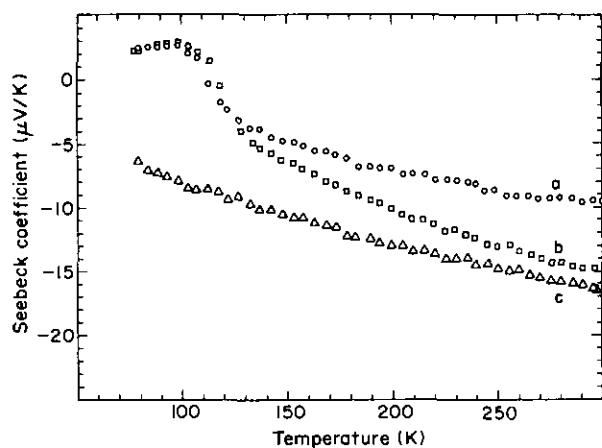


FIG. 6. Temperature-dependent Seebeck coefficient of (a) $\text{La}_3\text{Ni}_2\text{O}_7$, (b) $\text{La}_4\text{Ni}_3\text{O}_{10}$, and (c) LaNiO_3 .

ments of Seebeck coefficients for the $n = 2, 3$ members. Despite the rather significant variations in resistivity among the various members of the homologous series, the $S(T)$ variations of these compounds are almost the same. This feature is currently not properly understood. One explanation involves a complicated Fermi surface in the central Brillouin zone with several types of electron and hole pockets, the contributions of which to S nearly cancel out. The Fermi surface topology would then not be very sensitive to n . Such a situation could arise from the complexities of the crystal structure and/or from the overlap of the O $2p$ and Ni $3d$ bands. All the samples exhibit a negative S value at higher temperatures ($T > 100$ K), suggesting that electrons are the majority charge carriers. However, the Seebeck coefficients of the $n = 2$ and 3 members show a crossover to a positive value around 110 K. These data suggest that charge transport in the $n = 2$ and 3 members of the series involves both electrons and holes, while for the $n = \infty$ member it involves primarily electrons. In the case of the $n = 3$ mem-

ber, a change of slope in the S versus T plot is observed at $T \sim 130$ K, where a change of slope in the ρ versus T plot is also noted. The change in the slope of the $n = 2$ member is less pronounced. Furthermore, the Seebeck coefficients at room temperature tend to become more negative with increasing n and decreasing resistivity. This suggests that, with increasing n , an increasing fraction of electrons become itinerant and contribute to the charge transport process. The thermopower of La_2NiO_4 , which exhibits semiconducting resistivity behavior, is known to be positive at low temperatures (10).

The electronic properties of different members of the $\text{La}_{n+1}\text{Ni}_n\text{O}_{3n+1}$ series can be rationalized in terms of a schematic band model shown in Fig. 7. We have not indicated the position of the O $2p$ band separately but have indicated schematically the position of the hybridized Ni $3d_{x^2-y^2, z^2}$ and O $2p$ band, since both the Ni $3d$ and O $2p$ derived states may partially overlap. In La_2NiO_4 , the antibonding Ni e_g band, which is half filled, is split into a lower (full) and an upper (empty) subband, due to the large intra-atomic Coulomb interaction between the charge carriers. This splitting takes place regardless of whether the material is a Mott-Hubbard or a charge transfer compound. For strictly stoichiometric material the Fermi level lies in the middle of the band gap. In this case the charge transport is thermally activated at low temperatures, a feature which has been verified in recent infrared reflectivity measurements (41). However, at higher temperatures, where $k_B T$ approaches the band gap

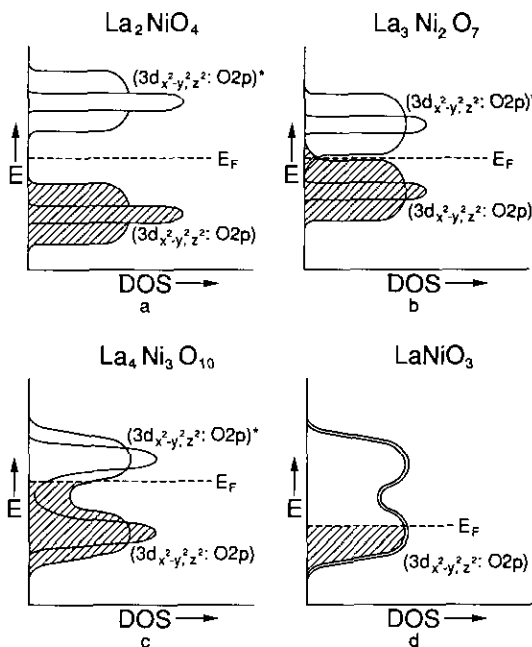


FIG. 7. Schematic band diagram proposed for (a) $n = 1$, (b) $n = 2$, (c) $n = 3$, and (d) $n = \infty$ members of the $\text{La}_{n+1}\text{Ni}_n\text{O}_{3n+1}$ series.

energy, gap closure occurs, which leads to an I-M transition. This could equally occur if the gap were of the charge transfer type. It is assumed to zero order that this particular band structure is not appreciably altered as n is increased. Then, with sufficiently large carrier density and n , the Fermi level is expected to shift into the lower subband. However, when the carrier density is low, narrow midgap states develop, which would result in an increase in the density of states at the Fermi level, as well as in an increase in the Ni d -band width (W). The observed trend in the temperature dependence of the resistivity and Seebeck coefficient with an increase in n is consistent with this picture. Furthermore, the $\rho(T)$ and the $\chi(T)$ results for the $n = 2$ and 3 members, which have a nonintegral valence, suggest that in this regime charge transport is dominated by strong electron-electron ($e-e$) interactions and by valence fluctuations. Fluctuating-valence behavior is observed when the levels corresponding to two different charge configurations (such as d^n and d^{n+1}) are close in energy and coexist close to the Fermi level. In the present case such a situation could arise from the energetically proximate levels of $3d^7$ and $3d^8$ electronic configurations associated with the $\text{Ni}^{3+}/\text{Ni}^{2+}$ valence states or from charge transfer effects. This corresponds to the coexistence of a relatively broad $3d_{x^2-y^2}$ and a relatively narrow $3d_{z^2}$ band at the Fermi level, as shown in Fig. 7. Here, the possible interaction between the essentially "itinerant" electrons of $3d_{x^2-y^2}$ parentage and the nearly "localized" electrons of $3d_{z^2}$ parentage would lead to conduction-electron localized moment scattering. This results in large values of the resistivity, as well as in weak localization effects such as are observed for the intermediate members. However, low-temperature heat capacity and structural data will be needed to draw more definitive conclusions on the low-temperature transport properties of these compounds. For the $n = \infty$ member the resistivity data at low temperatures show a T^2 dependence (12) characteristic of strong $e-e$ interaction in the three-dimensional Fermi liquid.

In conclusion, electrical resistivity, magnetic susceptibility, and thermopower measurements on the $n = 2, 3$, and ∞ members of the $\text{La}_{n+1}\text{Ni}_n\text{O}_{3n+1}$ series have been carried out on air-annealed samples. Together with the known properties of the $n = 1$ member La_2NiO_4 , a progressive decrease in the electrical resistivity and a change-over from semiconducting to metallic-like behavior are observed with an increase in n across this series. The $\rho(T)$ behavior of the $n = 2$ and 3 members is interpreted in terms of weak localization, which we attribute to the presence of conduction-electron (hole) localized moment scattering. By contrast, LaNiO_3 is metallic, with a T^2 dependence at low temperatures which is characteristic of electron scattering effects in a three-dimensional Fermi

liquid. The Seebeck data suggest that charge transport takes place via both electrons and holes in the case of the $n = 2$ and 3 members, but through electrons in the $n = \infty$ member. The $\chi(T)$ behavior of the $n = 2$ and 3 members is similar to that of the valence-fluctuation systems, and the $n = \infty$ member behaves like a Pauli paramagnet with strong electron-electron interactions. These results suggest that while the $n = 1$ member is in the small polaron limit, the $n = 2$ and 3 members, which are close to the transition boundary between insulating and metallic regimes, show evidence of fluctuating-valence behavior that might be linked to charge transfer effects. With a further increase in n , a crossover to a metallic phase occurs, which has properties characteristic of a strongly correlated Fermi liquid.

ACKNOWLEDGMENT

The authors acknowledge support of research by MISCON under Grants DOE DE-FG02-90ER 45427 and NSF-INT 9204467.

REFERENCES

- See, for example, the articles in "Electronic Properties of High- T_c Superconductors and Related Compounds" (H. Kuzmany, M. Mehring, and J. Fink, Eds.) Springer-Verlag, New York/Berlin 1990).
- M. Seppanen, *Scand. J. Metall.* **8**, 191 (1979).
- J. C. Brisi, M. Vallino, and F. Abbattista, *J. Less-Common Met.* **79**, 215 (1981).
- J. Drenan, C. P. Tavares, and B. C. H. Steele, *Mater. Res. Bull.* **17**, 621 (1982).
- P. Odier, Y. Nigara, J. Coutures, and M. Sayer, *J. Solid State Chem.* **56**, 32 (1985).
- S. N. Ruddlesden and P. Popper, *Acta. Crystallogr.* **11**, 54 (1958).
- C. N. R. Rao, D. Buttrey, N. Otsuka, P. Ganguly, H. R. Harrison, C. J. Sandberg, and J. M. Honig, *J. Solid State Chem.* **51**, 266 (1984).
- K. K. Singh, P. Ganguly, and J. B. Goodenough, *J. Solid State Chem.* **52**, 254 (1984).
- P. Ganguly and C. N. R. Rao, *Mater. Res. Bull.* **8**, 405 (1973).
- M. Sayer and P. Odier, *J. Solid State Chem.* **67**, 26 (1987).
- R. A. Mohan Ram, L. Ganapathi, P. Ganguly, and C. N. R. Rao, *J. Solid State Chem.* **63**, 139 (1986).
- K. Sreedhar, J. M. Honig, M. Darwin, M. McElfresh, P. Shand, J. Xu, B. Crooker, and J. Spalek, *Phys. Rev. B* **46**, 6382 (1992).
- M. Hervieu, C. Michel, A. Maignan, C. Martin, and B. Raveau, *J. Solid State Chem.* **74**, 428 (1988).
- G. Aeppli and D. J. Buttrey, *Phys. Rev. Lett.* **61**, 203 (1988).
- T. Freltoft, D. J. Buttrey, G. Aeppli, D. Vaknin, and G. Shirane, *Phys. Rev. B* **44**, 5046 (1991).
- R. R. Schartman and J. M. Honig, *Mater. Res. Bull.* **24**, 671 (1989).
- P. Gopalan, M. W. McElfresh, Z. Kakol, J. Spalek, and J. M. Honig, *Phys. Rev. B* **45**, 249 (1992).
- J. Lawrence, *Phys. Rev. B* **20**, 3770 (1979).
- Y. Ueda, K. Kosuge, and S. Kachi, *Mater. Res. Bull.* **12**, 763 (1977).
- B. F. Griffing, S. P. Faile, and J. M. Honig, *Phys. Rev. B* **21**, 154 (1980).
- S. Nagata, P. H. Keesom, and S. P. Faile, *Phys. Rev. B* **20**, 2886 (1979).
- M. O'Keeffe and F. S. Stone, *J. Phys. Chem. Solids* **23**, 261 (1962).
- M. Kato, Y. Mano, and T. Fujita, *Physica C* **176**, 533 (1991).
- R. J. Cava, B. Batlogg, T. T. Palstra, J. J. Krajewski, W. F. Peck, Jr., A. P. Ramirez, and L. W. Rupp, Jr., *Phys. Rev. B* **43**, 1229 (1991).
- P. Kuiper, G. Kruizinga, J. Ghijsen, G. A. Sawatzky, and H. Verweij, *Phys. Rev. Lett.* **62**, 221 (1989).
- P. Kuiper, J. van Elp, G. A. Sawatzky, A. Fujimori, S. Hosoya, and D. M. de Leeuw, *Phys. Rev. B* **44**, 4570 (1991).
- T. Mizokawa, H. Namatame, A. Fujimori, K. Akeyama, H. Kondo, H. Kuroda, and N. Kosugi, *Phys. Rev. Lett.* **67**, 1638 (1991).
- J. B. Torrance, P. Lacorre, C. Asavaroengchai, and R. M. Metzger, *J. Solid State Chem.* **90**, 168 (1991).
- J. B. Torrance, P. Lacorre, A. I. Nazzal, E. J. Ansaldo, and Ch. Niedermayer, *Phys. Rev. B* **45**, 8209 (1992).
- M. Medarde, A. Fontaine, J. L. García-Muñoz, J. Rodríguez-Carvajal, M. de Santis, M. Sacchi, G. Rossi, and P. Lacorre, *Phys. Rev. B* **46**, 14975 (1992).
- J. Zaanen, S. A. Sawatzky, and J. W. Allen, *Phys. Rev. Lett.* **55**, 418 (1985).
- N. Y. Vasanthacharya, P. Ganguly, J. B. Goodenough, and C. N. R. Rao, *J. Phys. C: Solid State Phys.* **17**, 2745 (1984).
- P. Ganguly, N. Y. Vasanthacharya, C. N. R. Rao, and P. P. Edwards, *J. Solid State Chem.* **54**, 400 (1984).
- K. P. Rajeev, N. Y. Vasanthacharya, A. K. Raychaudhuri, P. Ganguly, and C. N. R. Rao, *Physica C* **153-155**, 1331 (1988).
- J. G. Bednorz and K. A. Müller, *Rev. Mod. Phys.* **60**, 585 (1988).
- K. P. Rajeev, G. V. Shivashankar, and A. K. Raychaudhuri, *Solid State Commun.* **79**, 591 (1991).
- P. Lacorre, J. B. Torrance, J. Pannetier, A. I. Nazzal, P. W. Wang, and T. C. Huang, *J. Solid State Chem.* **91**, 225 (1991).
- Y. Takeda, R. Kanno, M. Sakano, O. Yamamoto, M. Takano, Y. Bando, H. Akinaga, K. Takita, and J. B. Goodenough, *Mater. Res. Bull.* **25**, 293 (1990).
- K. Sreedhar and C. N. R. Rao, *Mater. Res. Bull.* **25**, 1235 (1990).
- C.-J. Liu, M. D. Mays, D. O. Cowan, and M. G. Sanchez, *Chem. Mater.* **3**, 495 (1991).
- Xiang-Xin Bi, P. C. Eklund, E. McRae, Ji-Guang Zhang, P. Metcalf, J. Spalek, and J. M. Honig, *Phys. Rev. B* **42**, 4756 (1990).